

Toward understanding the depletion of two-level systems in ultrastable glasses

Wencheng Ji^{1,2,3}

¹*Institute of Physics, École Polytechnique Fédérale de Lausanne (EPFL), CH-1015 Lausanne, Switzerland*

²*Department of Physics of Complex Systems, Weizmann Institute of Science, Rehovot 76100, Israel*

³*School of Engineering and Applied Sciences, Harvard University, Cambridge, Massachusetts 02138, USA*

The density of Two-level systems (TLS) controls the low-temperature thermal properties in glasses and has been found to be almost depleted in ultrastable glasses. While this depletion of TLS is thought to have a close relationship with the dramatic decrease of quasi-localized modes (QLMs), it has yet to be clearly formalized. In this work, we argue, based on the *soft-potential* model, that TLS correspond to QLMs with typical frequency ω_0 . The density n_0 of TLS is proportional to both the density of QLMs $D_L(\omega_0)$, and the fraction of symmetric double-wells $f(\omega_0)$ at ω_0 , i.e., $n_0 \propto D_L(\omega_0)f(\omega_0)$. We numerically estimate ω_0 and n_0 in computer glasses at different levels of stabilities, and find that ω_0 is about 5% to 10% of the Debye frequency. n_0 in ultrastable glasses is over 1000 times smaller than that in poorly prepared glasses, with both $D_L(\omega_0)$ and $f(\omega_0)$ decreasing significantly. Remarkably, the order of magnitude of estimations for n_0 agrees with that found in experiments in amorphous silicon. Our study paves the way to understanding the depletion of TLS through the rarefaction of QLMs.

Introduction: In glasses, an atom or a group of atoms can tunnel between two nearby energy wells, which corresponds to the switch between two energy states called two-level systems (TLS) [1]. Although the entities of TLS are still not clear, the phenomenological *tunneling* TLS model proposed by Anderson et al. [2] and Phillips [3] successfully explains the abnormal thermal properties in glasses around 1 Kelvin (K), whose specific heat is approximately linear in temperature T and thermal conductivity almost proportional to T^2 [4]. In many previous studies, the density of TLS n_0 has been found to be nearly constant [5–8]. However, thanks to the state-of-art vapor deposition method by which ultrastable glasses can be prepared in experiments, the specific heat around 1 K in such glasses is found to be proportional to T^3 [9, 10]. This finding implies that n_0 decreases significantly in ultrastable glasses [11], which is also supported by the latest numerical simulations where n_0 decreases by a factor of 100 [12]. However, n_0 in these simulations is still two orders of magnitude greater than the experimental results. From a theoretical perspective, the role of interactions between TLS, which influences n_0 , is still widely debated [13–16]. On the practical aspect, it is essential to reduce n_0 because TLS cause decoherence in superconducting qubits which are a promising candidate for the construction of quantum computers [17–19].

n_0 is related to the concentration of double-well potentials (DWPs), and the latter is thought to be linked to the density of local vibrational modes, namely, quasi-localized modes (QLMs) since DWPs have large spatial overlaps with some fraction of QLMs [14, 20, 21]. QLMs (normal modes of the Hessian) are present at low-frequency vibrational spectrum [22] and can be easily obtained nowadays in computer glasses. In most glasses, the density of QLMs has the form $D_L(\omega) = A_4\omega^4$ for small frequency ω [23–30]. The prefactor A_4 is also found to decrease by several hundreds of times in ultrastable

glasses compared to poorly prepared glasses [29]. However, the origin of QLMs, specifically the dramatic decrease of A_4 is debated [31, 32]. Moreover, the quantitative relationship between A_4 and n_0 is unclear.

In this paper, we argue, based on the *soft-potential* model, that TLS correspond to the QLMs with typical frequency ω_0 . Their density n_0 is proportional to both $D_L(\omega_0)$ and the fraction of symmetric DWPs $f(\omega_0)$ at ω_0 , as shown in Fig. 1 with a sketch. We numerically estimate ω_0 and n_0 in computer glasses at different levels of stabilities. We find that ω_0 is about 5% to 10% of the Debye frequency, and n_0 in ultrastable glasses is more than 1000 times smaller than poorly prepared glasses, with both $D_L(\omega_0)$ and $f(\omega_0)$ playing a significant role. Remarkably, the order of magnitude of estimations for n_0 agrees with that found in experiments in amorphous silicon.

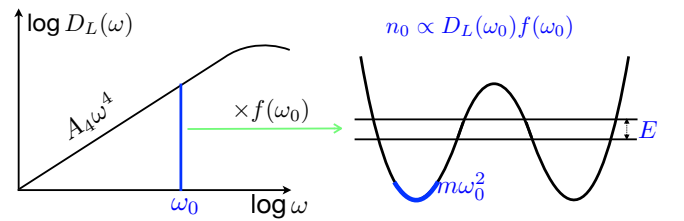


Figure 1. Sketch of the relationship between the density of TLS n_0 and QLMs $D_L(\omega)$. $D_L(\omega) = A_4\omega^4$ for small ω (left); symmetric DPWs along the reaction coordinate with the energy splitting $E \sim k_B K$, which corresponds to a near-constant curvature $m\omega_0^2$ at minima for a given system preparation (right), where m is the mass of the particle and k_B is the Boltzmann constant. Since the reaction coordinate that is curvilinear is along the direction of QLMs around the minimum [21], TLS correspond to the QLMs with frequency ω_0 . Their density $n_0 \propto D_L(\omega_0)f(\omega_0)$ where $f(\omega_0)$ reflects the fraction of symmetric DWPs.

Model: We follow the spirit of the *soft-potential* model [33–35] by which the local potential of double wells along the reaction coordinate s can be written approximately to the fourth-order of the Taylor expansion around a minimum. This local potential reads

$$U(s) = \frac{1}{2}m\omega^2 s^2 + \frac{\kappa}{3!}s^3 + \frac{1}{4!}\chi s^4, \quad (1)$$

where m is the mass of a particle with equal mass. We assume that the curvilinear reaction coordinate [36] is along the direction of QLMs around the minimum, which is supported by Ref. [21]. ω thus corresponds to an eigenfrequency of the QLMs. Physically, $\chi > 0$ which ensures that the potential has a lower energy limit. Due to the numerical observation that χ is narrowly distributed [24], χ is set to be a constant for a given system preparation and becomes larger in more stable glasses [37]. κ is set to be positive without loss of generality [38]. The joint density distribution $P(\omega, \kappa)$ is given by

$$P(\omega, \kappa) = \frac{1}{3N} \sum_i \sum_j \delta(\omega - \omega_i) \delta(\kappa - \kappa_j). \quad (2)$$

where N is the number of particles in a three-dimensional glass, ω_i and κ_j are the discrete values of ω and κ .

In the quantum tunneling regime, the DWPs are of near equal depth which indicates $\kappa \approx \kappa_c \equiv \omega\sqrt{3m\chi}$. According to the *tunneling* TLS model [2, 3], the energy splitting $E = ((\delta\varepsilon)^2 + \Delta_0^2)^{1/2}$ where $\delta\varepsilon$ is energy asymmetry and Δ_0 is the tunneling contribution derived from the WKB approximation. Δ_0 reads

$$\Delta_0 \approx W \exp \left[- \int_{s_1}^{s_2} \frac{\sqrt{2mU(s)}}{\hbar} ds \right] = W \exp \left[- \left(\frac{\omega}{\bar{\omega}} \right)^3 \right] \quad (3)$$

where $s_{1,2} = -2\kappa_c/\chi$, 0, are two minima of the symmetric double well. $\bar{\omega} = (\hbar\chi/(2m^2))^{1/3}$. W is a characteristic energy and we adopt $W = \hbar(\hbar\chi/(96m^2))^{1/3}$ same with the choice in Ref. [39]. Note that Δ_0 is insensitive to the change of W compared to ω .

Now we can obtain the joint density distribution $P(E, \Delta_0)$ in the vicinity of symmetric wells from $P(\omega, \kappa)$ where $\kappa = \kappa_c + \delta\kappa$ and $\delta\kappa \ll \kappa_c$.

$$P(E, \Delta_0) = P(\omega, \kappa) \left\| \frac{d\omega d\kappa}{dE d\Delta_0} \right\| \approx P_0 \frac{E}{\Delta_0 \sqrt{E^2 - \Delta_0^2}} \quad (4)$$

where

$$P_0 = \frac{P(\omega, \kappa_c) \kappa_c}{18\hbar} \left(\frac{\bar{\omega}}{\omega} \right)^6. \quad (5)$$

In the above calculation (see detail in Support Information (SI)), we considered the leading order of κ around κ_c , that is $P(\omega, \kappa) \approx P(\omega, \kappa_c)$ where $P(\omega, \kappa_c)$ indicates the density of modes with symmetric wells.

Δ_0 has a lower bound $\Delta_{\min} \approx 10^{-13} k_B K$. It corresponds to the experimental time scale $\tau \sim 100$ s [40]. At large Δ_0 (small ω), P_0 would be proportional to $[\ln(W/\Delta_0)]^{-2/3}$ since $P(\omega, \kappa_c)$ is argued to be proportional to ω^3 [20, 39] [41]. Since P_0 decreases with decreasing Δ_0 , it weakens the contributions of $P(E, \Delta_0)$ at tiny Δ_0 compared to regarding P_0 as a constant. The lower bound Δ_{\min} would play a less significant role than the upper bound E . For example, from a simple numerical calculation, $\int_{\Delta_{\min}}^{10\Delta_{\min}} P(E, \Delta_0) d\Delta_0$ is about 6 times smaller than $\int_{0.1E}^E P(E, \Delta_0) d\Delta_0$ that is about 24% of the total integral value, where we use $W = 10E$. The former integral could be further smaller if $P(\omega, \kappa_c)$ is saturated at tiny Δ_0 (large ω). From Eq. (3), ω is narrowly distributed [42]. Hence, taking all the above factors into account, we think that TLS correspond to a typical frequency for a given system preparation:

$$\omega_0 = \left[\ln \left(\frac{W}{E} \right) \right]^{1/3} \bar{\omega}, \quad (6)$$

which is obtained by setting to $\Delta_0 = E$ in Eq. (3). From the above equation, ω_0 is insensitive to the magnitude of E where $E \sim k_B T$ at low temperature [1]. The existing typical ω_0 is verified in the recent numerical work [21].

To integrate Δ_0 out in Eq. (4) to get $P(E)$, we set to $\Delta_0 = E$ in P_0 since it varies slowly compared to $1/(\Delta_0 \sqrt{E^2 - \Delta_0^2})$ and will not change the order of magnitude of the integral [43]. Also note that the conventional definition of the density of TLS $n_0(E) \equiv 3NP(E)/V$ is the number of TLS per volume per energy [5]. At last, $n_0(E)$ reads

$$n_0(E) \approx \frac{P(\omega_0, \kappa_0) \kappa_0}{6\hbar a^3} \ln^{-2} \left(\frac{W}{E} \right) \ln \left(\frac{2E}{\Delta_{\min}} \right), \quad (7)$$

where $\kappa_0 = \omega_0 \sqrt{3m\chi}$ and $a \equiv (V/N)^{1/3}$ is the interparticle distance. Considering that $P(\omega_0, \kappa_0) \kappa_0 \propto [\ln(W/E)]^{4/3}$ also depends on E , $n_0(E)$ varies slowly with varying E . Hence, from this place, we set to $E = 1k_B K$ [44] to estimate the density of TLS $n_0(E = k_B K)$ (n_0 for short):

$$n_0 = C_0 P(\omega_0, \kappa_0) \kappa_0, \quad (8)$$

where $C_0 \approx \frac{31}{6\hbar a^3} \ln^{-2}(W/k_B K)$. The value of Δ_{\min} is assigned. For a given material, C_0 is insensitive to the system preparation since a and the logarithmic term slightly change. Therefore the change of the magnitude of n_0 is determined by $P(\omega_0, \kappa_0)$. Once we know the value of $P(\omega_0, \kappa_0)$, we can get n_0 . However, to get the reaction coordinates, also called minimum energy paths (MEPs), is computationally very expensive [21]. We estimate $P(\omega_0, \kappa_0) \kappa_0$ in another simple way.

Qualitatively, $P(\omega_0, \kappa_0) \kappa_0$ is directly related to the density of QLMs $D_L(\omega_0)$. But only the fraction of QLMs

$f(\omega_0)$ correspond to DWPs with symmetric wells since QLMs also correspond to single wells and for DWPs just a fraction of them are symmetric DWPs. To build up the relation, we rewrite

$$P(\omega_0, \kappa_0) \kappa_0 = D_L(\omega_0) f(\omega_0), \quad (9)$$

where

$$f(\omega_0) \equiv \frac{P(\omega_0, \kappa_0) \kappa_0}{\int_0^\infty P(\omega_0, \kappa) d\kappa}. \quad (10)$$

Note that $D_L(\omega) \equiv \int_0^\infty P(\omega, \kappa) d\kappa = \frac{1}{3N} \sum_i \delta(\omega - \omega_i)$, which includes both single wells and double wells [45]. We will see later that $D_L(\omega_0)$ can be calculated exactly and dimensionless $f(\omega_0)$ can be estimated by a way.

We have no restriction on the form of $D_L(\omega_0)$ with respect to ω_0 up to now. In a regular glass, $D_L(\omega_0) = A_4 \omega_0^4$ still holds at ω_0 (see the discussion in next section). Therefore,

$$n_0 \propto A_4 \quad (11)$$

It explains why n_0 has a dramatic decrease with decreasing parent temperatures [12] since A_4 dramatically decreases with it as well below some typical temperature [28, 29]. If there are no double wells (only single wells), regardless of the magnitude of $D_L(\omega_0)$, $n_0 = 0$ because of $f(\omega_0) = 0$. Hence, both $D_L(\omega_0)$ and $f(\omega_0)$ influence the magnitude of n_0 [46].

Numerical estimation: We estimate the values of n_0 in three-dimensional zero-temperature computer glasses that are quenched instantaneously from equilibrated configurations at four parent temperatures $T_p = 0.8, 0.55, 0.35, 0.3$. The glass transition temperature T_g is about 0.5. See the model detail in [47]. Here, ten thousand equilibrated configurations at each T_p ($T_p = 0.55, 0.35, 0.3$) at $N = 2000$ prepared by the SWAP Monte Carlo method [48] are taken from [29]. Equilibrated configurations with 1000 realizations at $T_p = 0.8$ at $N = 8000$ are prepared by the normal molecular dynamics method directly.

The typical frequency ω_0 depends on W and $\bar{\omega}$ both of which are as a function of χ . We let $\chi = c_1 m \omega_D^2 / a^2$ where ω_D is the Debye frequency. Dimensionless c_1 is estimated numerically. The typical frequency ω_0 obtained from Eq. (6) can be expressed as

$$\frac{\omega_0}{\omega_D} = \left[\frac{c_1 \hbar}{2m\omega_D a^2} \ln \left(\frac{\hbar\omega_D}{k_B K} \left(\frac{c_1 \hbar}{96m\omega_D a^2} \right)^{\frac{1}{3}} \right) \right]^{\frac{1}{3}}. \quad (12)$$

ω_0 is approximately proportional to $c_1^{1/3}$. We know that $m\omega_D^2 a^2$ is an order of the banding energy 10 eV and $\hbar\omega_D \sim 50$ meV because the Debye temperature is usually several hundred Kelvin. If $(c_1/2)^{1/3}$ is of order 1, as a rough estimation, $\omega_0 \sim 0.1\omega_D$.

To do the careful calculations of ω_0 , $D_L(\omega_0)$ and $f(\omega_0)$, we explicitly adopt the parameters of the amorphous silicon where $m = 4.8 \times 10^{-26}$ kg and $a = 2.9 \times 10^{-10}$ m [49]. ω_D at different T_p is slightly different because the elastic moduli increase with decreasing T_p . We set to $\omega_D = 530 k_B K / \hbar$ [50] at $T_p = 0.55$ since it is close to the glass transition temperature. See SI how we estimate $\omega_D(T_p)$ at the other three T_p . Specifically, $c_1 \approx 0.5, 0.8, 2.1, 2.5$ from high to low T_p , which is taken from the median of $\chi_1 / (m\omega_D^2 / a^2)$ (see the definition of χ_1 later). As a result, $\omega_0 / \omega_D \approx 0.06, 0.07, 0.94, 0.10$ (listed in TABLE I.) is consistent with our rough estimations above. $\omega_0 / \bar{\omega}$ are about 1.24, 1.27, 1.33, 1.34, which is less insensitive to the system preparation as we expect from Eq. (6).

In such computer glasses, the density of QLMs has a pseudogap at low frequency $D_L(\omega) = A_4 \omega^4$. The upper bound of this scaling regime is about 20% to 30% of ω_D [29]. So the quartic spectrum of QLMs at ω_0 holds although they would be hybridized with the plane waves. We extract A_4 from $D_L(\omega)$ (see SI) for small ω and then get $D_L(\omega_0) = A_4 \omega_0^4$.

To estimate $f(\omega_0)$, we Taylor expand local potentials along the non-linear modes (also called ‘cubic modes’) [51, 52] which capture the local energy landscapes better. See SI for the detail of non-linear modes. We thus get the coefficients ω_1 , κ_1 , and χ_1 . Note that χ_1 (or c_1) is insensitive to the Taylor expansion along non-linear modes or normal modes (see SI). Fig. 2 shows the scatter of $\kappa_1 / (\sqrt{\chi_1} \omega_D)$ vs. ω_1 / ω_D at four T_p we have. From Eq. (10), we first estimate the numerator $P(\omega_0, \kappa_0)$ by calculating the average density $P(\omega, \kappa)$ between the green line and the red dashed line in the range $\omega_1 / \omega_D \in [0.04, 0.16]$ (between two green bars) instead of at κ_0 and ω_0 . Then the denominator $\int_0^\infty P(\omega_0, \kappa) d\kappa$ in Eq. (10) is averaged in this ω_1 range as well. The green line $\kappa_1 / \sqrt{\chi} = \sqrt{3} \omega_1$ corresponds to the two wells with equal depth and the red dashed line $\kappa_1 / \sqrt{\chi} = \sqrt{8/3} \omega_1$ corresponds to the spinodal case according to our model [20]. See the estimated $f(\omega_0)$ in Table I. We tested that the order of magnitude of $f(\omega_0)$ will not change if we choose a narrower range of ω_1 at three higher T_p . At the lowest $T_p = 0.3$, we only find two points in the integral interval and $f(\omega_0)$ strongly depends on the range we choose. However, the estimations of $D_L(\omega_0)$ and C_0 are reliably and they are smaller at lower T_p , and they ensure the decrease of n_0 . The dramatic decrease in $f(\omega_0)$ because of the higher proportion of single wells (dots below the spinodal line in Fig. 2) is consistent with the recent findings that DWPs are rarer than QLMs in ultrastable glasses [21, 52].

From the above estimations, C_0 is insensitive to the system preparation. Both $D_L(\omega_0)$ and $f(\omega_0)$ decrease significantly with lowering T_p which leads to the significant decrease in n_0 by a factor of over 1000. The estimated n_0 agrees with the experimental

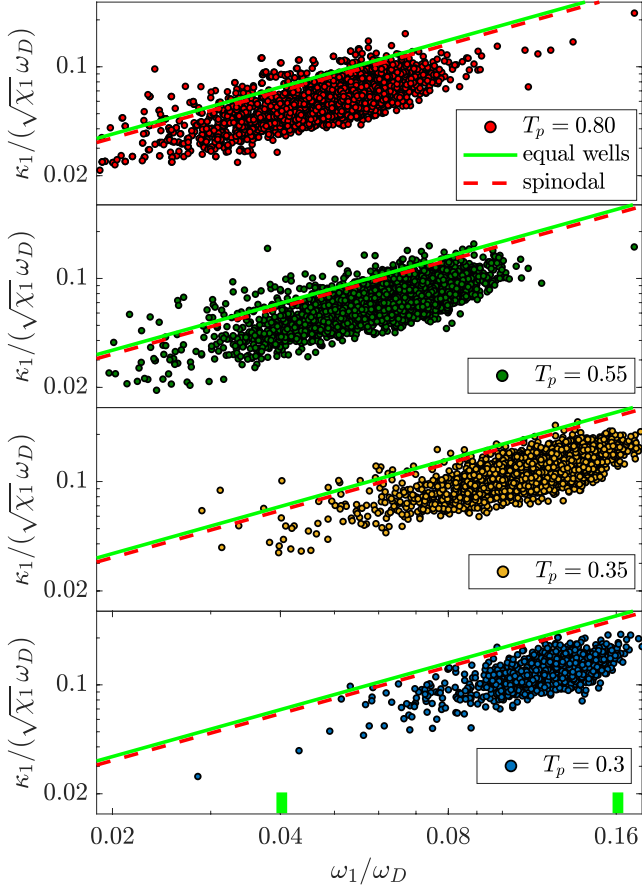


Figure 2. Scatter of $\kappa_1/(\sqrt{\chi}\omega_D)$ vs. ω_1/ω_D for non-linear modes at four T_p . The green curve $\kappa_1/\sqrt{\chi} = \sqrt{3}\omega_1$ indicates the symmetric double wells and the red dashed curve $\kappa_1/\sqrt{\chi} = \sqrt{8/3}\omega_1$ indicates the spinodal case according to our model [20]. A higher proportion of dots below the red dashed line is found at low T_p .

T_p	ω_0/ω_D	$C_0[(\text{Jm}^3\text{s})^{-1}]$	$D_L(\omega_0)[\text{s}]$	$f(\omega_0)$	$n_0[\text{J}^{-1}\text{m}^{-3}]$
0.80	0.06	5.4×10^{62}	5.3×10^{-15}	0.36	1.0×10^{48}
0.55	0.07	4.8×10^{62}	3.8×10^{-16}	0.26	4.7×10^{46}
0.35	0.94	3.7×10^{62}	2.5×10^{-16}	0.05	4.2×10^{45}
0.30	0.10	3.5×10^{62}	5.9×10^{-17}	0.03	6.1×10^{44}

Table I. The estimations of ω_0 , C_0 , $D_L(\omega_0)$, and $f(\omega_0)$ at four T_p in amorphous silicon. The density of TLS $n_0 = C_0 D_L(\omega_0) f(\omega_0)$ decreases dramatically with lowering T_p .

measurement of n_0 in amorphous silicon which varies between $10^{45} - 10^{48} \text{ J}^{-1}\text{m}^{-3}$ [49].

Conclusion We have built up the quantitative relationship between the density of TLS and the density

of QLMs. We found that (i) TLS which contribute to the thermal transport, correspond to the QLMs with frequency ω_0 that is about 5% to 10% of ω_D ; (ii) The decrease in the density of TLS n_0 is not only influenced by the rarefaction of the density of QLMs $D_L(\omega_0)$ but also influenced by the decrease of $f(\omega_0)$. The latter reflects the distribution of local energy landscapes; (iii) The estimations of n_0 are consistent with that found in experiments in amorphous silicon. Although we relied on several assumptions and even some of them are inaccurate (see the discussion below), we think that for the order of magnitude of n_0 , our method is effective since we grasped the properties of key parameters ω_0 , $D_L(\omega_0)$ and $f(\omega_0)$ in n_0 .

The previous work [14] argues that TLS are dominated by the lower bound Δ_{\min} , which corresponds to the longest experimental time τ , to explain some universality in glasses. However, we think that TLS are dominated by the tunneling whose time scale is much smaller than τ . Because of the successful estimations on the dramatic decrease in n_0 and the right order of ω_0/ω_D that is supported by the recent work [21] where a more careful calculation for the tunneling is considered, our picture appears to be closer to the prediction of TLS in experiments [49].

The estimated n_0 in our approach in most stable glasses is more than 100 times smaller than that in [12]. Indeed, the quartic potentials (Eq.(1)) and nonlinear modes we adopted do not accurately describe the DWPs according to their numerical results, but we think it will not change the order of magnitude of n_0 . One may think that they overestimated n_0 by using the classical thermal activations to probe the DWPs since most of TLS they found corresponding to long tunneling times (lower bound of Δ_0) will not be found in experiments. However, it is not the case since the order of magnitude of n_0 is insensitive to changing the lower bound of Δ_0 according to our argument. The main source of discrepancy of n_0 might be that the system they used is different (particle density, pair interaction) which leads to that A_4 [28] varies less significantly than the Ref. [29] that we used.

It is worth noting that, besides Ref.[12, 21], some other works [53–57] also probe the DWPs directly, and some of them look at the properties of DWPs along the MEPs to estimate n_0 numerically. Clearly, we can get n_0 from Eq.(8) once we get $P(\omega_0, \kappa_0)$ through MEPs. Due to lack of simulation technology on MEPs, we cannot compare n_0 in this way to our results.

Admittedly, in our adopted approach the estimation on $f(\omega_0)$ is not precise, but we believe that $f(\omega_0)$ decreasing with lowering T_p should be correct, and that, at least at high T_p , $f(\omega_0)$ we estimated is a good approximation. $f(\omega_0)$ would be proportional to the ratio of C_{TLS}/C_{sm} , where $C_{\text{TLS}} \propto n_0$ and $C_{sm} \propto D_L(\tilde{\omega})$ with typical $\tilde{\omega}$ are the prefactors of specific heat contributions for TLS and local harmonic oscillators, respectively. This ratio is in-

deed found to be smaller in experiments in more stable amorphous material B_2O_3 [58].

In the latest work [37], the geometry of low-energy local excitations (local rearrangements) is systemically studied where the local excitations become more localized in more stable glasses. It would be interesting to verify it on tunneling particles [12]. If that is true, then the first-principles calculations, for example, Path Integral Molecular Dynamics method [59], in real materials would be possible, which might reveal the entities of TLS in the end.

To explain the rarefaction of QLMs (dramatic decrease of A_4), Ref. [31] proposes a thermal excitations picture that is controlled by a typical frequency, and Ref. [32] uses an interacting harmonic oscillators model with some controlling parameters. But a third model (or picture) using the parameters that can be measured directly in computer glasses to explain the behavior of A_4 quantitatively is needed. Since A_4 reflects the level of the stability of glasses, the understanding of A_4 would shed light on developing a new method to prepare more stable computer glasses in the future.

Acknowledgments. We thank E. Bouchbinder, A. Kumar, I. Procaccia, T.W.J. de Geus, F. Zamponi, and Y. Zheng for useful discussions, and M. Wyart for useful discussions in the whole process. We thank F. Zamponi for some specific suggestion. We thank the authors of [29] for providing us with equilibrated swap configurations. We also thank the Simons Collaboration on Cracking the Glass Problem which provides a great platform to exchange knowledge and form the initial idea of this work.

-
- [1] W. Phillips, *Reports Prog. Phys.* **50**, 1657 (1987).
 - [2] P. Anderson, B. Halperin, and C. Varma, *Philos. Mag.* **25**, 1 (1972).
 - [3] W. Phillips, *Journal of Low Temperature Physics* **7**, 351 (1972).
 - [4] R. Zeller and R. Pohl, *Phys. Rev. B* **4**, 2029 (1971).
 - [5] W. A. Phillips and A. Anderson, *Amorphous solids: low-temperature properties*, Vol. 24 (Springer, 1981).
 - [6] J. Freeman and A. Anderson, *Physical Review B* **34**, 5684 (1986).
 - [7] J. Berret and M. Meissner, *Zeitschrift für Physik B Condensed Matter* **70**, 65 (1988).
 - [8] R. O. Pohl, X. Liu, and E. Thompson, *Reviews of Modern Physics* **74**, 991 (2002).
 - [9] T. Pérez-Castañeda, C. Rodríguez-Tinoco, J. Rodríguez-Viejo, and M. Ramos, *Proc. Natl. Acad. Sci.* **111**, 11275 (2014).
 - [10] X. Liu, D. R. Queen, T. H. Metcalf, J. E. Karel, and F. Hellman, *Physical review letters* **113**, 025503 (2014).
 - [11] M. A. Ramos, *Low Temperature Physics* **46**, 104 (2020).
 - [12] D. Khomenko, C. Scalliet, L. Berthier, D. R. Reichman, and F. Zamponi, *Physical Review Letters* **124**, 225901 (2020).
 - [13] C. Yu and A. Leggett, *Comments on Condensed Matter Physics* **14**, 231 (1988).
 - [14] D. A. Parshin, H. R. Schober, and V. Gurevich, *Phys. Rev. B* **76**, 064206 (2007).
 - [15] V. Lubchenko and P. Wolynes, *Annu. Rev. Phys. Chem.* **58**, 235 (2007).
 - [16] L. Faoro and L. B. Ioffe, *Phys. Rev. B* **91**, 014201 (2015).
 - [17] J. Martinis, K. Cooper, R. McDermott, M. Steffen, M. Ansmann, K. Osborn, K. Cicak, S. Oh, D. Pappas, R. Simmonds, and C. Yu, *Phys. Rev. Lett.* **95**, 210503 (2005).
 - [18] F. Arute, K. Arya, R. Babbush, D. Bacon, J. C. Bardin, R. Barends, R. Biswas, S. Boixo, F. G. Brandao, D. A. Buell, et al., *Nature* **574**, 505 (2019).
 - [19] C. Müller, J. H. Cole, and J. Lisenfeld, *Reports on Progress in Physics* **82**, 124501 (2019).
 - [20] W. Ji, M. Popović, T. de Geus, E. Lerner, and M. Wyart, *Phys. Rev. E* **99**, 023003 (2019).
 - [21] D. Khomenko, D. R. Reichman, and F. Zamponi, *Physical Review Materials* **5**, 055602 (2021).
 - [22] H. Schober, C. Oligschleger, and B. Laird, *J. Non. Cryst. Solids* **156-158**, 965 (1993).
 - [23] M. Baity-Jesi, V. Martín-Mayor, G. Parisi, and S. Perez-Gavero, *Physical review letters* **115**, 267205 (2015).
 - [24] E. Lerner, G. Düring, and E. Bouchbinder, *Phys. Rev. Lett.* **117**, 035501 (2016).
 - [25] H. Mizuno, H. Shiba, and A. Ikeda, *Proc. Natl. Acad. Sci.* **114**, E9767 (2017).
 - [26] E. Lerner and E. Bouchbinder, *J. Chem. Phys.* **148**, 214502 (2018).
 - [27] M. Shimada, H. Mizuno, M. Wyart, and A. Ikeda, *Phys. Rev. E* **98**, 060901 (2018).
 - [28] L. Wang, A. Ninarello, P. Guan, L. Berthier, G. Szamel, and E. Flenner, *Nat. Commun.* **10**, 26 (2019).
 - [29] C. Rainone, E. Bouchbinder, and E. Lerner, *Proc. Natl. Acad. Sci.* **117**, 5228 (2020).
 - [30] E. Lerner and E. Bouchbinder, *The Journal of Chemical Physics* (2021).
 - [31] W. Ji, T. W. J. de Geus, M. Popović, E. Agoritsas, and M. Wyart, *Phys. Rev. E* **102**, 062110 (2020).
 - [32] C. Rainone, P. Urbani, F. Zamponi, E. Lerner, and E. Bouchbinder, *SciPost Physics Core* **4**, 008 (2021).
 - [33] M. A. Ilyin, V. G. Karpov, and D. A. Parshin, *Zh. Eksp. Teor. Fiz.* **92**, 291 (1987).
 - [34] Y. M. Galperin, V. Karpov, and V. Kozub, *Advances in Physics* **38**, 669 (1989).
 - [35] D. Parshin, *Physical Review B* **49**, 9400 (1994).
 - [36] The reaction coordinate that connects two well is the path of minimum energy.
 - [37] W. Ji, T. W. de Geus, E. Agoritsas, and M. Wyart, *arXiv preprint arXiv:2106.13153* (2021).
 - [38] If $\kappa < 0$, flip the sign of it by using $-s$ without changing ω^2 and χ .
 - [39] D. Parshin, *Phys. Scr.* **T49A**, 180 (1993).
 - [40] Δ_{\min} is estimated by $\Delta_{\min} = \hbar\pi/\tau$.
 - [41] At very tiny Δ_0 , $P(\omega, \kappa_c)$ might be near-constant or might (dramatically) decrease by increasing ω .
 - [42] When $W = 10E$, ω is 2.4 times larger at Δ_{\min} than that at $\Delta_0 = E$.
 - [43] If we adopt $P_0 \propto [\ln(W/\Delta_0)]^{-2/3}$, then the integral is approximately 3 times smaller when $W = 10E$.
 - [44] If $E = 10k_B K$, $P(E)$ only increases by around 70% compared to $E = k_B K$ where we use $W = 100k_B K$.

- [45] Since single wells do not correspond to reaction coordinates, this part of integral can be calculated along directions of QLMs in Eq.(10). It will not change the value of the integral. Of course, if we know that which QLMs correspond to DWPs, we know minimum energy paths and directly use Eq. (8).
 - [46] In [60], the authors think that the density of QLMs for the part of DPWs is proportional to ω^3 which is incompatible with our consideration if $D_L(\omega) \sim \omega^4$ for small ω , which is argued in our previous work [20].
 - [47] E. Lerner, *Journal of Non-Crystalline Solids* **522**, 119570 (2019).
 - [48] A. Ninarello, L. Berthier, and D. Coslovich, *Physical Review X* **7**, 021039 (2017).
 - [49] D. Queen, X. Liu, J. Karel, T. Metcalf, and F. Hellman, *Phys. Rev. Lett.* **110**, 135901 (2013).
 - [50] M. Mertig, G. Pompe, and E. Hegenbarth, *Solid State Commun.* **49**, 369 (1984).
 - [51] L. Gartner and E. Lerner, *Physical Review E* **93**, 011001 (2016).
 - [52] G. Kapteijns, D. Richard, and E. Lerner, *Physical Review E* **101**, 032130 (2020).
 - [53] F. Demichelis, G. Viliani, and G. Ruocco, *PhysChemComm* **2**, 20 (1999).
 - [54] J. Reinisch and A. Heuer, *Physical Review B* **70**, 064201 (2004).
 - [55] J. Reinisch and A. Heuer, *Physical review letters* **95**, 155502 (2005).
 - [56] T. Damart and D. Rodney, *Physical Review B* **97**, 014201 (2018).
 - [57] H. Mizuno, M. Shimada, and A. Ikeda, *Physical Review Research* **2**, 013215 (2020).
 - [58] M. A. Ramos, *Philosophical Magazine* **84**, 1313 (2004).
 - [59] D. Marx and M. Parrinello, *The Journal of chemical physics* **104**, 4077 (1996).
 - [60] A. Kumar, I. Procaccia, and M. Singh, *Europhysics Letters* (2021).
-

Supporting information – Toward understanding the depletion of two-level systems in ultrastable glasses

Calculation of the Jacobian $\left\| \frac{d\omega \wedge d\kappa}{dE \wedge d\Delta_0} \right\|$

To calculate the Jacobian $\left\| \frac{d\omega \wedge d\kappa}{dE \wedge d\Delta_0} \right\|$, we first calculate the energy difference $\delta\varepsilon$. For a double-well potential, $U(s) = \frac{1}{2}m\omega^2 s^2 + \frac{\kappa}{6}s^3 + \frac{1}{24}\chi s^4$, the positions of two minima are $s_0 = 0$ and $s_0 = \frac{-3\kappa - 3\sqrt{\kappa^2 - 8m\omega^2\chi/3}}{2\chi}$. The energy difference of two minima is

$$\delta\varepsilon = \frac{\left(3\kappa + \sqrt{9\kappa^2 - 24m\omega^2\chi}\right)^2 \left(-3\kappa^2 + 12m\omega^2\chi - \kappa\sqrt{9\kappa^2 - 24m\omega^2\chi}\right)}{192\chi^3}. \quad (13)$$

Its derivative with respect to κ at κ_c is $\frac{d\delta\varepsilon}{d\kappa}|_{\kappa=\kappa_c} = \frac{4\kappa_c^3}{3\chi^3}$, where $\kappa_c = \sqrt{3m\chi}\omega$ (the symmetric double well condition). We also know $\delta\varepsilon = \sqrt{E^2 - \Delta_0^2}$ and $\Delta_0 = W \exp\left(-\left(\frac{\omega}{\bar{\omega}}\right)^3\right)$.

Then the Jacobian $\left\| \frac{d\omega \wedge d\kappa}{dE \wedge d\Delta_0} \right\|$ in the vicinity of symmetric wells is:

$$\begin{aligned} \left\| \frac{d\omega \wedge d\kappa}{dE \wedge d\Delta_0} \right\| &= \left| \frac{dE}{d\kappa} \frac{d\Delta_0}{d\omega} \right|^{-1} \\ &= \left| \frac{dE}{d\delta\varepsilon} \frac{d\delta\varepsilon}{d\kappa} \frac{d\Delta_0}{d\omega} \right|^{-1} \\ &\simeq \left[\frac{\delta\varepsilon}{E} \frac{4\kappa_c^3}{3\chi^3} \frac{3W}{\omega} \left(\frac{\omega}{\bar{\omega}}\right)^3 \exp\left(-\left(\frac{\omega}{\bar{\omega}}\right)^3\right) \right]^{-1} \\ &= \frac{\chi^3\omega}{4\kappa_c^3} \left(\frac{\bar{\omega}}{\omega}\right)^3 \frac{E}{\Delta_0 \sqrt{E^2 - \Delta_0^2}} \\ &= \frac{\kappa_c}{18\hbar} \left(\frac{\bar{\omega}}{\omega}\right)^6 \frac{E}{\Delta_0 \sqrt{E^2 - \Delta_0^2}} \end{aligned} \quad (14)$$

Estimation of the Debye frequency at different T_p

Numerically, we can estimate the Debye frequency by the formula $\omega_D(T_p) = [18\pi^2\rho/(2c_t^{-3} + c_l^{-3})]^{1/3}$. $\rho \equiv N/V$ is the particle number density which is a constant; $c_t = \sqrt{G/(m\rho)}$ and $c_l = \sqrt{(B + 4G/3)/(m\rho)}$ are the transverse and longitudinal velocity, related to the shear modulus G and bulk modulus B ; m is the particle mass (taken equal for all particles). Once we set to $\omega_D(T_p = 0.55) = 530k_B K/\hbar$, we can calculate ω_D by

$$\omega_D(T_p) = \frac{530k_B K}{\hbar} \left[\frac{2G^{-3/2} + (B + 4G/3)^{-3/2}}{2G_0^{-3/2} + (B_0 + 4G_0/3)^{-3/2}} \right]^{-1/3}$$

where B_0 and G_0 are the values at $T_p = 0.55$. We do not need to worry the units of B (or G) since they are canceled. We get $\omega_D(T_p = 0.3) \approx 610k_B K$, $\omega_D(T_p = 0.35) \approx 590k_B K$, and $\omega_D(T_p = 0.8) \approx 500k_B K$.

Extract A_4 from $D_L(\omega)$ for small ω

We show the density of QLMs $D_L(\omega)\omega_D$ vs. ω/ω_D (both of which are dimensionless) for small ω in Fig. 3. Since $\int D(\omega) d\omega = 1$, we have $\int D(\omega)\omega_D d(\omega/\omega_D) = 1$. For small ω , $D(\omega)\omega_D = A_4\omega_D^5 (\omega/\omega_D)^4$ where the prefactor $A_4\omega_D^5$ is dimensionless as well. The black dashed lines indicate the fitted $D(\omega)\omega_D$ for small ω .

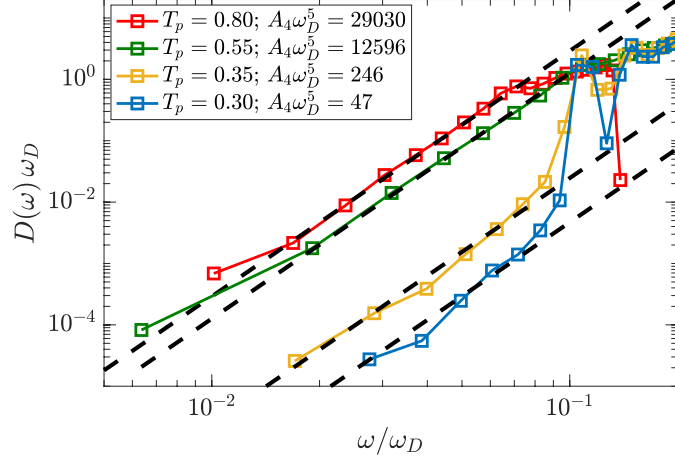


Figure 3. Density of normal modes $D(\omega)\omega_D$ vs ω/ω_D . $D(\omega) = D_L(\omega) = A_4\omega^4$ for small ω . $D(\omega)$ is calculated by $D(\omega) \equiv \langle \frac{1}{3N} \sum_i \delta(\omega - \omega_i) \rangle$, where $\langle \cdot \rangle$ stands for the ensemble average and ω_i is the discrete eigenfrequency of the Hessian matrix.

Non-linear modes

The non-linear modes \vec{z}_f can be obtained by minimizing the cost function by applying the steepest descent method that starts from the QLMs directions. The cost function [51, 52] is

$$F = \frac{|U^{(3)} \bullet \vec{z}\vec{z}\vec{z}|^2}{|H \bullet \vec{z}\vec{z}|^3}$$

where z is initially along the QLMs directions. Note that F does not depend on the magnitude of z and F is proportional to the energy barrier when the system is close to the instability. The total interaction $U = \sum_i \sum_{j>i} \varphi$ where φ is the pair interaction potential. $U^{(3)} = \frac{\partial^3 U}{\partial \vec{r} \partial \vec{r} \partial \vec{r}}$ and $H = \frac{\partial^2 U}{\partial \vec{r} \partial \vec{r}}$ where H is the Hessian matrix. \bullet means the contraction. Specifically

$$H: \vec{z}\vec{z} = \sum_{i<j} \left[\left(\frac{\varphi''}{|r_{ij}|^2} - \frac{\varphi'}{r_{ij}^3} \right) (\vec{r}_{ij} \cdot \vec{z}_{ij})^2 + \frac{\varphi'}{r_{ij}} (\vec{z}_{ij} \cdot \vec{z}_{ij}) \right] \quad (15)$$

$$U^{(3)} \bullet \vec{z}\vec{z}\vec{z} = \sum_{i<j} \left\{ \left(\frac{\varphi'''}{|r_{ij}|^3} - 3 \frac{\varphi''}{|r_{ij}|^4} + 3 \frac{\varphi'}{|r_{ij}|^5} \right) (\vec{r}_{ij} \cdot \vec{z}_{ij})^3 + \left(\frac{\varphi''}{|r_{ij}|^2} - \frac{\varphi'}{|r_{ij}|^3} \right) 3 (\vec{r}_{ij} \cdot \vec{z}_{ij}) (\vec{z}_{ij} \cdot \vec{z}_{ij}) \right\} \quad (16)$$

φ''' (φ'' , φ') is third (second, first) derivative of the pair interaction with respect to r_{ij} . The coefficients $\lambda_1, \kappa_1, \chi_1$ thus are obtained by the Taylor expansion of the potential U along z_f . Nonlinear modes in Fig. 2 in main text are obtained from QLMs whose frequencies are below the frequency of the first plane waves.

Estimation of c_1

We show the scatter plot of $\chi_1 a^2 / m \omega_D^2$ ($\chi a^2 / m \omega_D^2$) v.s. ω_1^2 (ω^2) for non-linear modes (QLMs) at four T_p . χ_1 is similar to χ for small ω at each T_p . We estimate c_1 from non-linear modes by taking the median value of $\chi_1 a^2 / m \omega_D^2$. Specifically, $c_1 \approx 0.5, 0.8, 2.1, 2.5$ from high to low T_p . The median of $\chi a^2 / m \omega_D^2$ obtained from QLMs for the lowest 50 softest QLMs (left side of the vertical lines) is approximately equal to 0.3, 0.6, 2.4, 2.3.

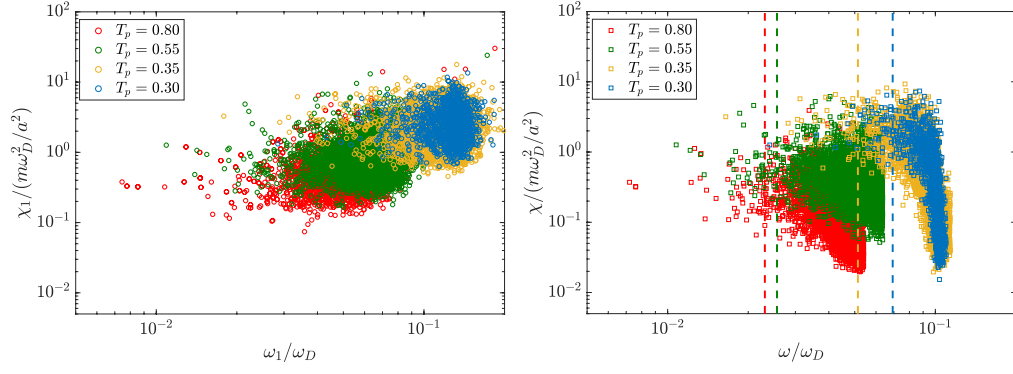


Figure 4. Scatter plots of $\chi_1 a^2 / m \omega_D^2$ vs. ω_1 / ω_D (left) and $\chi a^2 / m \omega_D^2$ v.s. ω / ω_D (right). For big ω , χ becomes smaller because QLMs are hybridized with plane waves. The vertical lines are the thresholds to estimate the median of $\chi a^2 / m \omega_D^2$.